Advances in Low-Cost Manufacturing and Folding of Solar Sail Membranes

Olive R. Stohlman,[1] Juan M. Fernandez,[1] Gregory D. Dean,[1] Nigel Schneider,[2] Jin Ho Kang,[3]
Randall Barfield[4], Taylor Herndon[5], and Peter Stokes[6]
NASA Langley Research Center, Hampton, VA 23681, USA

Solar sail membranes must have a high area-to-mass ratio and high solid volume fraction when stowed. In order to meet mission requirements, current solar sail projects, such as NASA's Near Earth Asteroid Scout, require metallized sail membranes with thicknesses on the order of 2-3 µm. These very thin membranes do not retain creases like thicker membranes, solar panels, or paper models. For Cubesat-class spacecraft, volume, rather than mass, is often the driving requirement for deployable structural elements. These two factors make it both difficult and highly desirable to characterize the practical differences between solar sail membrane packaging methods with laboratory demonstrations. This paper presents lessons gathered from lab work with solar sail membranes at a 10-meter scale.

I. Introduction

Solar sails are a form of propellantless space propulsion that generate thrust by reflecting sunlight with a large "sail." As this thrust is proportional to the area of the sail, the sail must be large and light weight. To launch, a sail must package to a volume that fits within a launch shroud; Cubesat-class solar sail demonstration missions like NEA Scout [1] aim to stow around 50 m^2/liter. The scale of this class of sail is illustrated in Figure 1, which shows a single triangular quadrant of an engineering prototype sail from the Advanced Composites-based Solar Sail System (ACS3) [2]. The long edge of this isosceles triangle is 9.2 m.

Figure 1: Folding a solar sail prototype triangular quadrant with a 9.2-meter edge for laboratory use.

Manufacturing a sail with an area of even 100 m^2 for laboratory use takes substantial floor space and effort. At the highest end, the NASA's Comet Halley rendezvous solar sail mission studies in 1977 included a report on scaling

[1] Research Aerospace Engineer, NASA Langley Research Center, Hampton, VA, AIAA member
[2] Design Engineer, AS&M TEAMS 3, Hampton, VA
[3] Associate Principle Engineer, National Institute of Aerospace, Hampton, VA, AIAA member
[4] Student Intern, Structural Dynamics Branch, NASA Langley Research Center
[5] Student, Oregon State University, Corvallis, OR
[6] Student, University of Connecticut, Storrs, CT

membrane production to the sail area requirements [2], noting that a fabrication facility of at least 20 by 5 m in a clean room would be required to manufacture the 8-by-7500-m heliogyro blades, with 26 months allocated for fabrication facility design, setup, and testing.

This paper presents some observations from laboratory work on a sail with a 9.2-meter edge. Section II is an overview of two basic sail designs and the materials selection rationale, with notes on the adhesive seaming methods. Section III addresses folding methods, folding patterns, and the volume impact of different fold patterns. In Section IV, two tests of the sail system are described: an ascent vent test and a rail deployment test, where the sail is pulled out of its spool by carriages sliding along fixed rails.

II. The ACS3 sail membrane design

The ongoing sail membrane work at NASA Langley Research Center supports the Advanced Composites-Based Solar Sail System (ACS3) project [3]. ACS3 is a solar sail demonstration concept for a 6U Cubesat satellite platform, meeting a standard Cubesat form factor of six 10-by-10-by-10-cm units. The stowed sail membrane system occupies approximately two liters of the spacecraft volume, and consists of two spools that each hold two triangular sail quadrants, which form the approximately 80 m^2 square sail. The sail membrane is pulled out of the spools by the solar sail's four deployable composite booms, where each boom tip extends one side of its two adjacent sail quadrants

The baseline design for the ACS3 solar sail membrane is a four-quadrant sail, where each quadrant is a right triangle with a long edge of 9.2 meters. The baseline sail material is 2-µm-thick polyethylene naphthalate (PEN, manufactured by Dupont-Teijin as Theonex), aluminized with a 100 nm thickness on the sun side to increase the reflectivity and coated with 15 nm of black chromium on the back side to increase the emissivity and keep the sail temperature to within operational limits. The metallized PEN film possesses similar maximum usage temperature (about 240°C) of LaRC^{TM} CP1 polyimide (fluorinated colorless polyimide, Nexolve) which was used for Nanosail-D and NEA Scout missions, and it has several benefits such as higher modulus (about 6 GPa vs. 2 GPa), higher tensile strength (over 190 MPa vs. 87 MPa), higher elongation at break (over 40% vs 2%) and lower price compared to the CP1 polyimide [4]. Early engineering prototypes were made of 2.5-µm-thick aluminized polyethylene terephthalate (PET, manufactured by Dupont-Teijin as Mylar), which has similar packaging and handling performance but is inexpensive. For these sails, the PEN material is cut from a roll that is 75 cm wide, so 13 gores are seamed together to produce a quadrant.

Sail assembly was done on a vacuum table with a cutting mat surface. This facilitates handling and alignment of the very thin sail sheets. To assemble the sail, 75-cm-wide gores of PEN (or PET) were seamed using 13 mm-wide 966 pressure-sensitive adhesive (PSA) transfer tape from 3M, which was chosen for its space heritage and wide operational temperature range. The 966 PSA is an acrylic based polymer and keeps about 50% level of room temperature adhesion strength up to 93°C. Edge reinforcements and ripstops, made of 966 PSA with aluminized Kapton backing, were then applied to the newly attached strip of material, and the edges were trimmed to the final sail shape before the next gore was attached.

Figure 2 shows the "A" design, which used pressure-sensitive adhesive tape to seam and reinforce the sail. This type of adhesive is suitable for use in multi-layer insulation [5] and is available in a variety of forms and with a variety of backing materials.

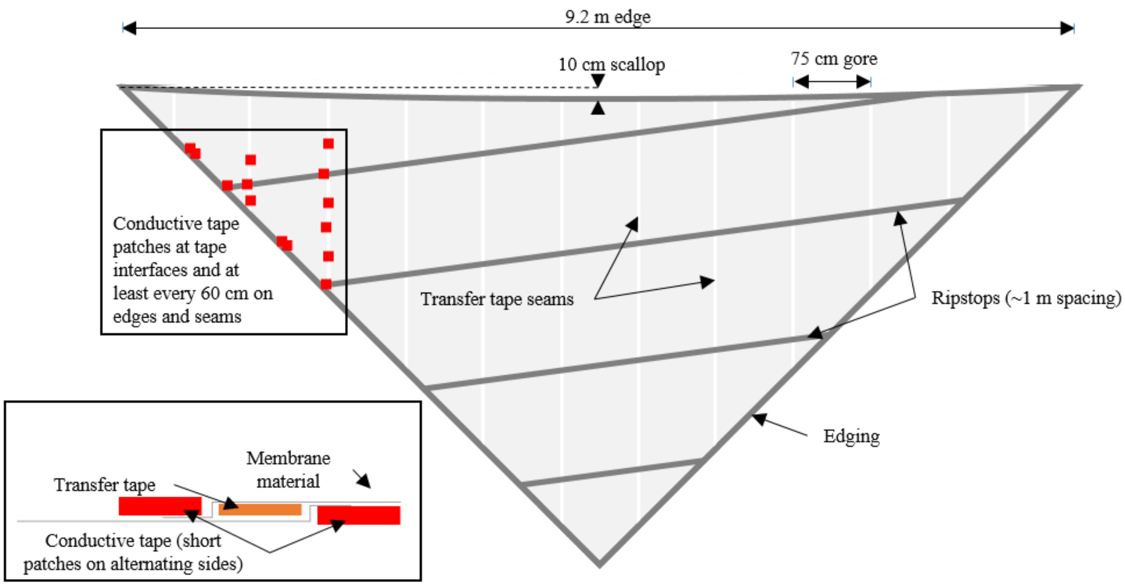

Figure 2: Sail design A with pressure-sensitive adhesive.

Conductive tape was included in the design to address the concern that an electrical charge could build up on one area of the sail and eventually arc to another part of the sail or spacecraft, or have an unexpected static charge effect on deployment. The inset in Figure 2 shows the approximate distribution of the conductive tape[7].

Because the metallized PEN (and PET) membrane was much thinner than the adhesive tapes used to seam the panels, the metallized PEN membrane contributed only about half of the total volume of the assembled sail. An approximate breakdown of the volume contribution of these different features is shown in Figure 3 and summarized in Table 1.

Table 1: Sail membrane volume by component for the ACS3 sail quadrants.

Edging backer	2%
Edging adhesive	10%
Seam adhesive	20%
Ripstop backer	3%
Ripstop adhesive	14%
Conductive backer	1%
Conductive adhesive	2%
Membrane	49%

[7] All tape was purchased from Dunmore Corp.

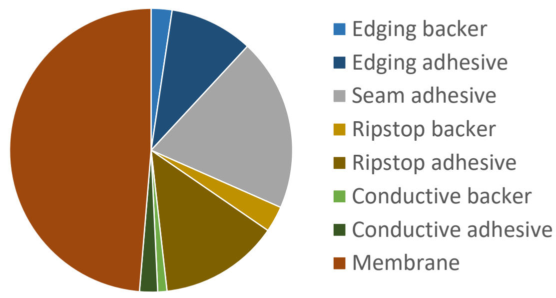

Figure 3: Volume contributions of the sail membrane material, tapes, and adhesives. The membrane material itself contributed about half of the volume of the assembled sail membrane; the remainder is dominated by tape adhesive. [3]

During testing, detailed in Section IV.D, the sail frequently adhered to itself at the edges of the tape and in places where adhesive residue was present. In some cases, the sail tore because of these adhesions. Unintended sticking was also a frequent problem during assembly and patching. While it is possible to mitigate these problems with pressure-sensitive adhesive by using a backing material that is wider than the adhesive layer, these problems motivated another approach to sail assembly.

Sail design B, shown in Figure 4, relied on changes to the folding pattern and a hot-melt adhesive, with two goals: to greatly reduce the use of pressure-sensitive adhesive and to improve packaging efficiency. Two hot-melt polyester web adhesives, Spunfab PA1811 with a 24 g/m^2 areal weight and Bostik PE165 of 14.5 g/m^2, were used, with similar results, to seam and edge a sail. PA1811 melts at approximately 75°C and PE165 melts at approximately 165°C, which are acceptable temperatures for use with PEN, which tolerates temperatures up to approximately 240°C [4]. The web was a thin sheet of unwoven matted plastic fiber and could be cut to shape with scissors or a blade.

Because of changes to the folding pattern, discussed further in Section III.B, the scalloped edge was removed from the design. The spacings of ripstops and conductive tape were increased to reduce volume. Otherwise, few changes were made between design A and design B.

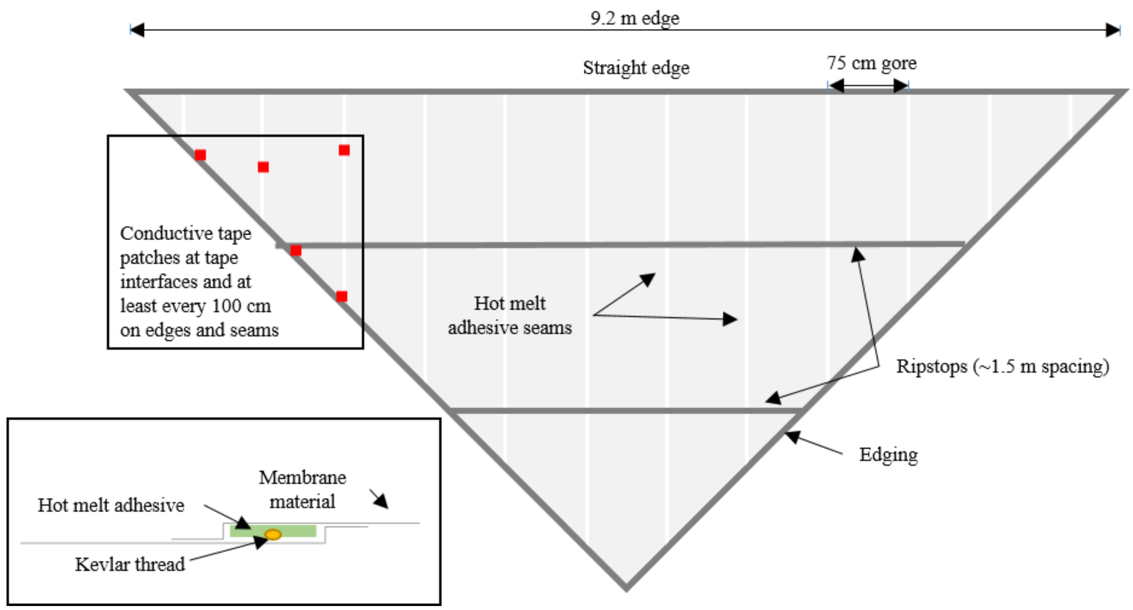

Figure 4: Sail design B with hot-melt adhesive.

The polyester web adhesive was melted using an iron with a digital temperature readout and a silicone-impregnated fiberglass cover. As shown in Figure 5, Kevlar string was sealed to the sail along seams and reinforcements, and the adhesive was covered with a strip of PEN so that no web adhesive is exposed on the sail. The quality of the seamed joint was characterized by a lap shear adhesion test method at room temperature. The test specimens were prepared according to a modified ASTM D5868. ASTM D5868 recommends 1 square inches adhesive area, but 0.5 inch by 3/8 inch (12.7 mm by 9.525 mm) adhesive area was employed due to the current sail design definition as shown in Figure 6 (a). When the specimen was stretched, the metallized PEN film just above the adhesive area was broken before the adhesive joint failed, which indicates the adhesion strength was higher than the tensile strength of the PEN membrane (Figure 6 (b)). The tensile load at break was about 4 N, and the stress on the sail membrane cross-section at the failure was calculated as about 154 MPa, which is higher than the biaxial tension level of deployed solar sails (about 0.007 MPa or 1 psi) (Figure 7). The adhesion strength at orbit conditions is under evaluation at different temperatures between -160°C and 120°C.

Figure 5: Ripstops on the sail were a stack of polyester web adhesive, Kevlar thread, and a cover of the membrane material. This stack was ironed to the membrane material, melting the web adhesive and fusing the layers.

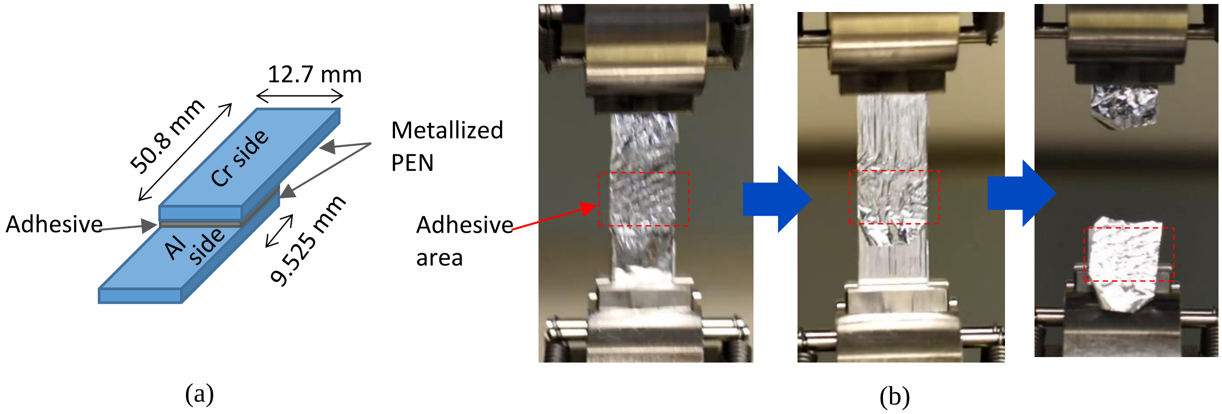

Figure 6: Adhesion test specimen dimensions (a) and images of membrane failure during an adhesion test (b).

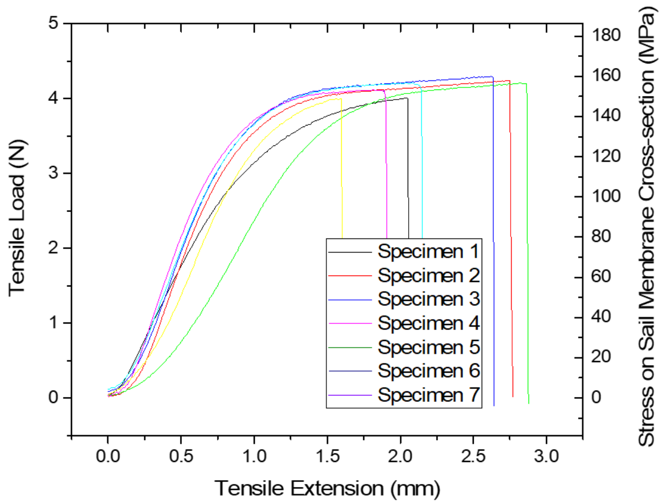

Figure 7: Tensile load at adhesion specimen failure and tensile stress on sail membrane cross-section at failure.

The sail corner fittings were aluminum sheet, fused with web adhesive to the sail membrane and covered with a second layer of PEN, as shown in Figure 8.

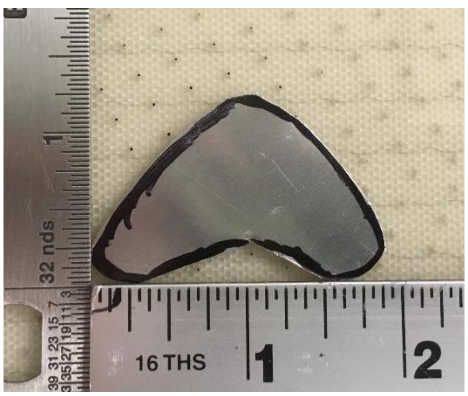

(a)

(b)

Figure 8: Sail corner fittings. The shape was cut from sheet metal (a) and sandwiched between the membrane and a PEN sheet (b) using hot-melt polyester web adhesive.

III.Sail membrane folding

The most straightforward way of folding a membrane is to fold it freehand, using a reference of some sort of fold height and maintaining the existing folds by pressing them under weights, magnets, or in clips. This can be time-consuming and the quality of the folds depends on the experience and care of the people doing the folding. At the other extreme, commercial folding machines are much faster and more repeatable, but require more resources to prepare and are limited in their possible patterns.

Folding along the long edge of the sail quadrant reduces the sail to a strip that can be wrapped about a spool, as shown in Figure 9. It is important to understand that membranes with a thickness on the order of 2.5 microns cannot be folded and handled like paper. Once folded, paper can be easily un-folded and re-folded along the original set of creases, but this is not true for a thin membrane material, which lacks the stiffness to maintain a localized fold. Once the membrane is folded, some management method is required to maintain the position of the folds as the folded strip is handled, as noted in Figure 9(a).

(a)

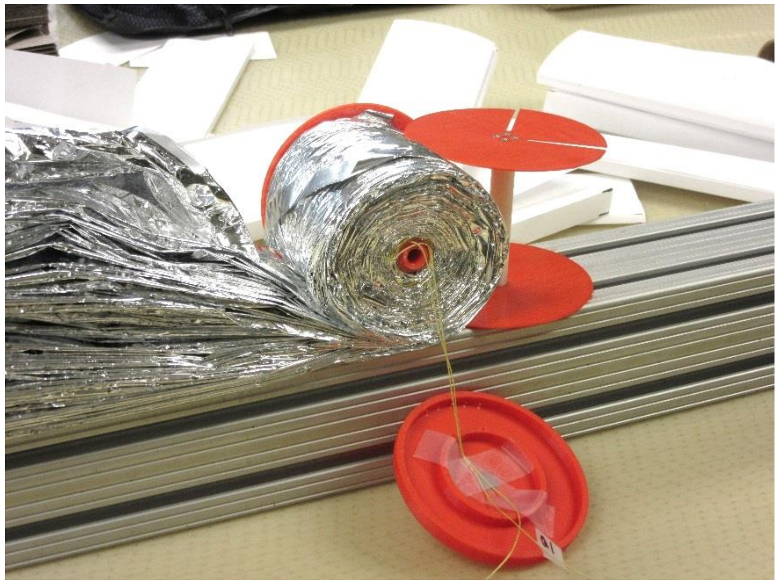

(b)

Figure 9: (a) Two z-folded PET sail quadrants. Paper forms were used to align folded edges during handling. (b) Partially wrapped sail quadrants. One spool flange was removed to show the wrapped sail.

A. Methods of folding

1. Folding between folding forms

The first folding method used for ACS3 lab work was folding between paper folding forms. This had the advantages of being fairly repeatable, less time-consuming than hand-folding a membrane, and allowing complex folding patterns. Two identical paper folding forms, such as those shown in Figure 10(a), were cut, with dashed or scored cuts at the intended fold lines. A perforating round blade was used to cut these dashed fold lines. For ACS3, large paper forms were manufactured by a computer-controlled Eastman cutting machine on a vacuum table. The membrane could be sandwiched between these two forms and the three layers were folded simultaneously, as in Figure 10(b-d).

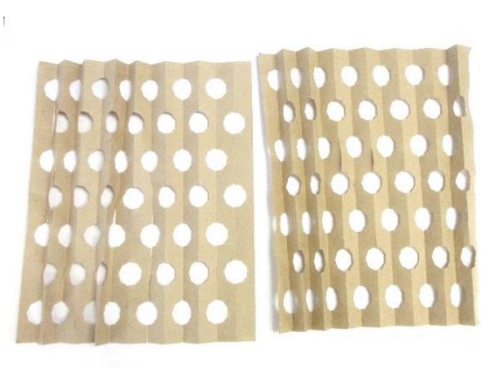

(a)

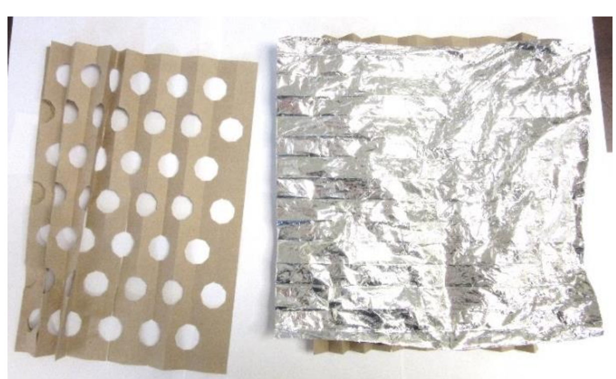

(b)

(c)

(d)

Figure 10: Folding a small section of PET membrane with paper forms.

After the membrane and the forms were folded together, it was challenging to remove the forms. This was made easier by including access notches in the folding forms, so the membrane could be pinched and restrained while the folding form was removed from one side, and then the other. This process is shown in Figure 11. At full scale, the folding forms were manufactured in sections that could be removed from the membrane one at a time. The full-scale folding process is shown in Figure 12.

(a)

(b)

(c)

(d)

(e) (f)

Figure 11: Removing the forms from the membrane. First (a), the membrane was pinched through an access hole in the paper folding form, shown in detail in (b). The paper folding form could be removed from one side (c). This operation was repeated to remove the other form (d) while restraining the membrane. The membrane was then free from its folding forms (e) and could be deployed (f).

This method of flat folding forms had some disadvantages. There were edges on the paper forms that could catch on the membrane, tearing it; it remained time-consuming to place and remove all the folding forms; new forms had to be re-manufactured if the fold pattern changed; the membrane did not perfectly fill the folding forms and thus had a slightly different final height. Despite these drawbacks, it took 1-2 days to fold the membrane with the forms and 4-6 days to fold it freehand.

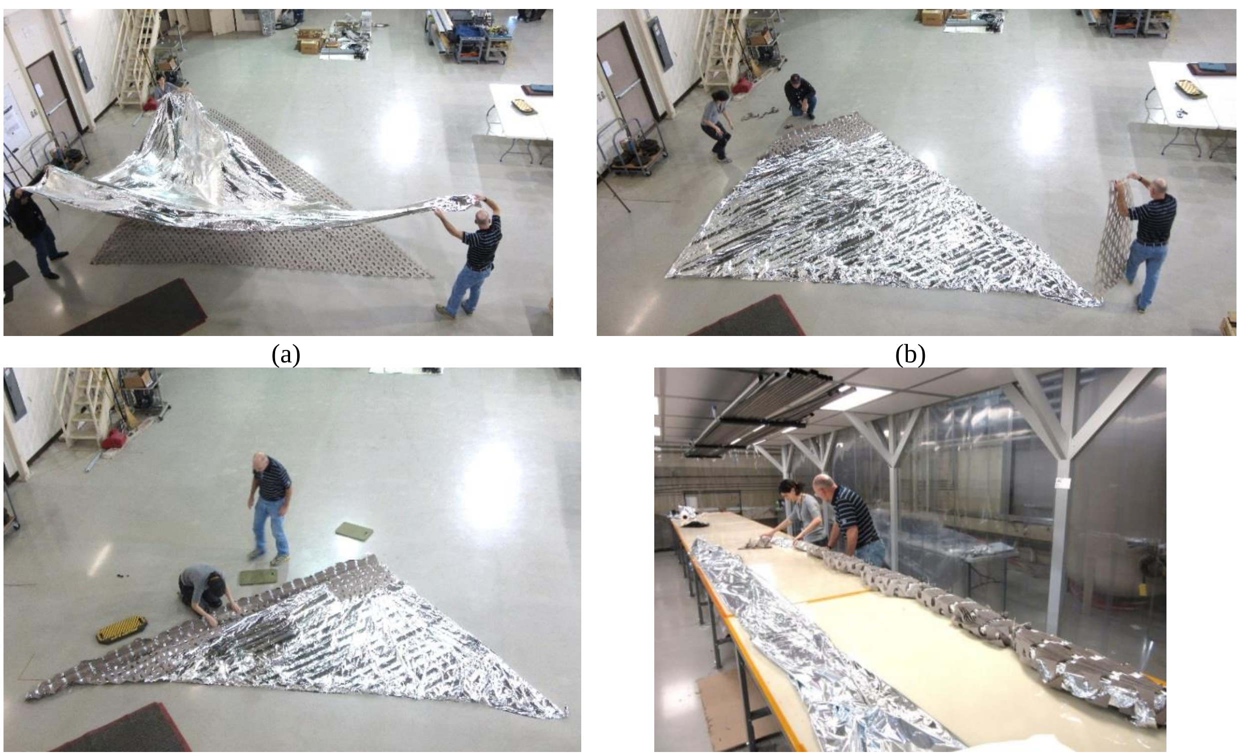

(a) (b)

(c) (d)

Figure 12: The folding process at full scale, for a sail quadrant with a 9.2-meter edge. The membrane was placed on a paper folding form (a), and the second folding form (b) was placed on top of the membrane in tiled sections. The membrane was gradually folded between the set of paper forms (c) as more sections were placed. Ultimately, the membrane and both paper forms were folded to the design size (d).

2. Folding in a channel

For a pattern without intersecting fold lines, a strict fold height could be enforced by folding the sail in a channel. As illustrated in Figure 13, a channel with smooth, straight sides at the same spacing as the fold height was set up on a table. Working from one end of the membrane, the first fold of the sail was placed in the channel and then covered with a strip of paper. The sail was folded back over this strip of paper, and the process was repeated. Paper strip could be removed from the lowest layer for reuse. Besides being easy to implement, this method positioned the folded sail conveniently for spooling, which reduced handling.

(a) (b) (c)

Figure 13: A piece of PET was folded in a channel by (a) placing the material in the channel, (b) placing a paper spacer in the channel, and (c) folding the membrane over the paper.

The channel folding guide was not well-suited for complex folds like the half-parallel z-fold shown in Figure 15(b), but it could be easily adjusted for the partial fan fold in Figure 15(c). Two full-scale PEN quadrants of design B were folded according to the partial fan fold pattern using a channel, with good results in folded height and improved speed over the paper folding forms.

3. Folding with local stiffness variation

When paper is folded and un-folded, it is easy to re-fold it along the same lines because the paper has been both plastically deformed and permanently softened at the fold lines. Thick plastic membranes are similarly easy to re-fold because of plastic deformation at the fold lines. With very thin materials, however, plastic deformation at a fold line is not sufficient to localize the fold to the same position.

Even very thin materials can be re-folded along the same lines if the material is entirely (as in Fernandez et al [6]) or partly (similarly to the method presented by Arya et al [7] for thick membranes) removed along the intended fold lines. This was discarded as an option for ACS3 because of the difficulty of cutting the PEN with a clean edge, but it is similarly possible to enforce repeatable fold lines by adding material on either side of the intended fold line.

Figure 14 shows a small PET quadrant with a long edge of 16 inches that was selectively reinforced with shaped pieces of tape. The segment was intended to be folded into a half-parallel z-fold, as in Figure 15(b). The membrane was naturally easier to fold along the gaps between patches of tape, which made the pattern easier to implement and prevented the folds from being disrupted by handling and rolling.

(a) (b) (c)

Figure 14: Localized differences in material stiffness could make folding much easier. This PET triangle had its edges reinforced with patches of Kapton tape, leaving gaps between the patches at intended fold lines (a). This allowed a half-parallel z-fold pattern (b) to be imposed very repeatably, so the piece was easily folded and refolded (c).

Adding material carried the disadvantage of stacking thicker material in one area. This method was not pursued at full scale because it was expected to require too much additional volume and development effort.

B. Trades between fold designs

Three families of fold patterns were considered, and are illustrated in Figure 15: entirely-parallel z-folds, half parallel z-folds, and partial fan folds. Entirely-parallel z-folds were the simplest option. Half-parallel z-folds meet at a fold along the sail centerline. In the partial fan fold, the folds near the sail center were slightly wedge-shaped, while the folds further from the center were parallel. All three of the illustrated fold patterns met the requirements of ACS3, but they were not all equally simple to implement, and they had different advantages when the folded sail was wrapped. Of the three, entirely parallel z-folds were the simplest to make, while the half-parallel z-folded patterns were the most difficult because of the folds along the centerline.

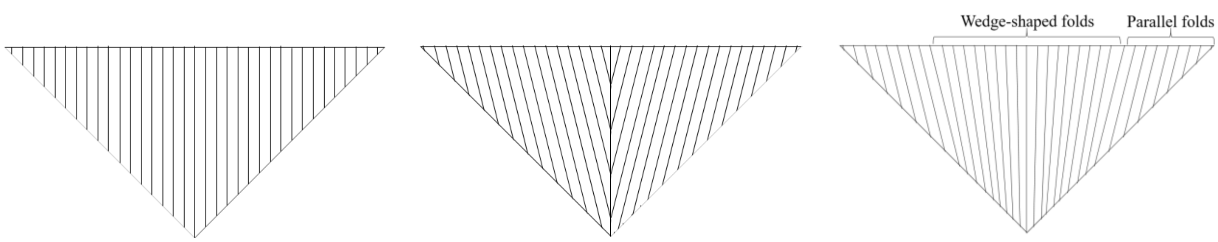

(a) Entirely-parallel z-fold (b) Half-parallel z-fold (c) Partial fan fold

Figure 15: Three families of fold patterns.

Three significant requirements were placed on the fold pattern:

1. It had to fold to a strip that could be spooled, as in Figure 16.
2. The maximum fold height had to be below 75 mm
3. The center corner had to fall at one end of folded strip and the outside corners at the other end

Several other features were identified as desirable:

1. Minimize stacking of thick features (ripstops, edging, and seams)
2. Ideally, folds should have been perpendicular to the sail edges (or at least not parallel), so that they would be pulled open by tension at the corners when the sail was fully deployed
3. Ideally, the last 1-2 wraps of material on the spool should have not been thick- that is, they should have had as few layers of material as possible (illustrated in Figure 17), to improve the neatness and symmetry of the spooled sail

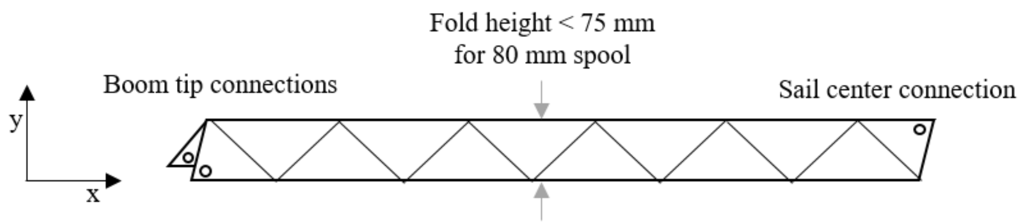

Figure 16: The folded sail strip and some of its requirements.

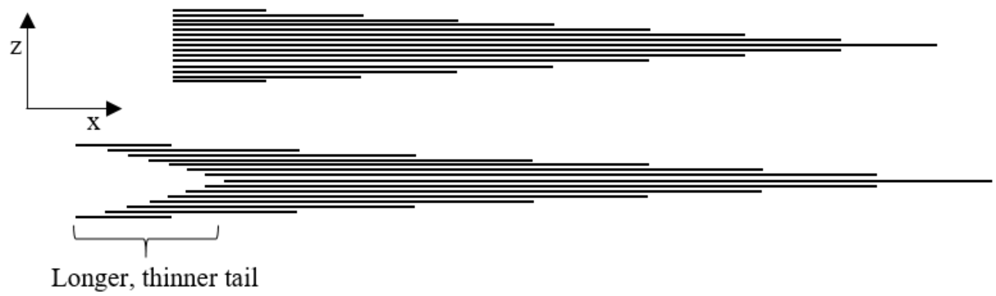

Figure 17: The folded sail strip (top view) showing how folded layers of a triangle stacked in entirely-parallel z-folds (above) and half-parallel z-folds or a partial fan fold (below).

The requirement that the corners of the sail had to be accessible to the boom and spool attachment points limited the possible angles at which the sail could be folded.

The entirely-parallel z-folded design was the initial baseline because it was simple to fold and expanded well during deployment. However, it produced a sail strip that was much thicker at one end than the other, as illustrated in Figure 17, and the sail was wrapped starting at the thinner end and proceeding to the thicker end. The final sail package then had a large lump in it, and was more difficult to handle and to restrain in a small volume. Scalloping the long edge of the sail produced a small improvement, but the improvement was in proportion to the sail area lost.

When determining the minimum dimensions of the sail spool and stowage volume, it was initially assumed that a sail with any fold height would occupy the same volume. We expected this to be approximately correct, but intuition also suggested that putting fewer folds in the sail would result in slightly more efficient packaging, as a thinner folded strip of sail was easier to wrap. A small study of folded and wrapped paper sheets was done to find the relationship between fold height and sheet area per stowed volume, expressed here as square meters of paper per cubic centimeter of rolled cylinder. The ACS3 packaging goal for a 2 µm-thick PEN sail with fittings was 0.06 m^2/cm^3; the paper in these cylinders was substantially thicker and packaged to around 0.01 m^2/cm^3.

After folding and wrapping 111 sheets of paper and Mylar of various dimensions at various fold heights with four different researchers, the primary finding was that freehand packaging efficiency was more strongly dependent on the skill of the person doing the folding and wrapping than on the fold height. Figure 18 shows some of the wrapped cylinders of paper, and Figure 19 presents the area per stowed volume of these wrapped cylinders.

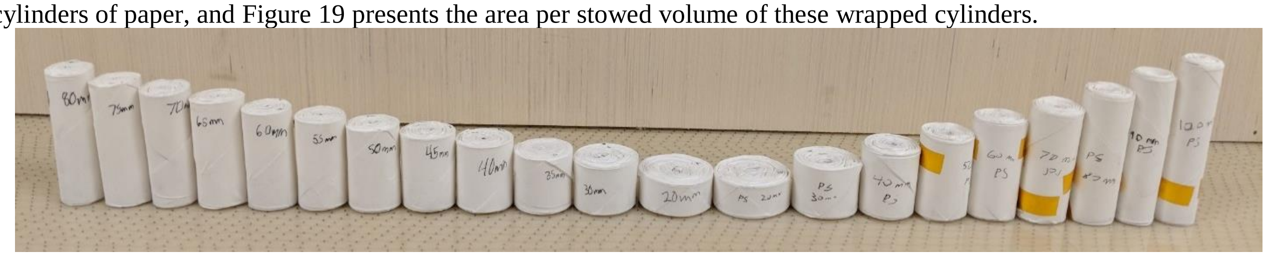

Figure 18: Entirely-parallel z-folded and cylindrically wrapped triangles of paper with different fold height and resulting wrapped diameters.

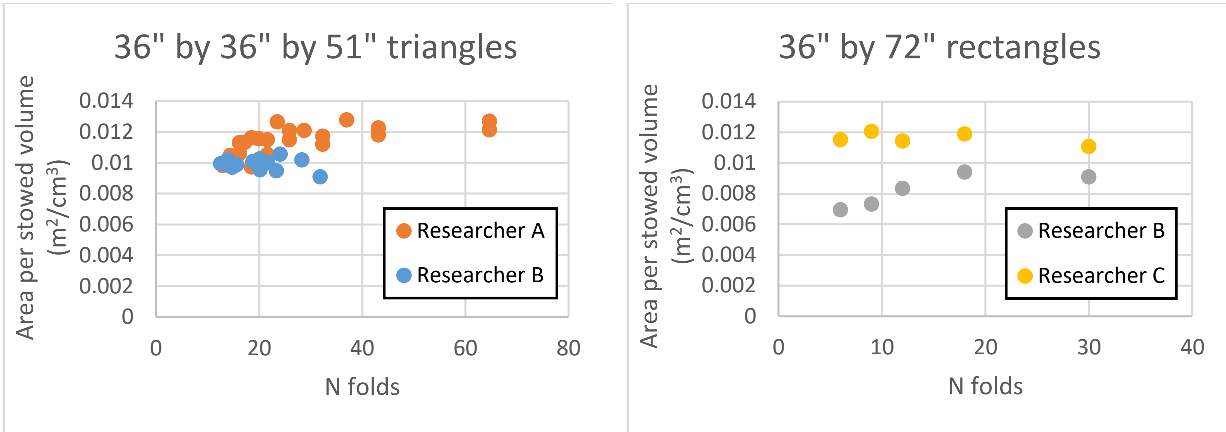

Figure 19: The area per stowed volume of entirely-parallel z-folded and spooled paper sheets.

It was also observed that the area per stowed volume of double-z-folded segments was similar to that of z-folded and wrapped segments, at around 0.012 m^2/cm^3 for the paper sheets, with a distinct dependence on the pressure with which the folded package was restrained [8] and no clear dependence on the height of the secondary z-fold. As illustrated by Figure 19, larger and smaller sheets of paper had similar packaging efficiencies.

IV.Sail membrane testing

C. Ascent venting

However tightly packaged, a folded membrane retains some air between layers of material. This raises the concern that, during spacecraft ascent, the retained air could be trapped by the membrane and inflate the stowed sail, damaging the membrane or nearby parts of the spacecraft. Ascent vent testing was performed on a PET prototype sail of design A wrapped on a 3D-printed spool with a 75-mm-wrapped-membrane-height to identify whether the decompression of the sail package would cause damage to the membrane or place a high load on any sail restraint mechanism that might later be added to the design.

A belt of clear plastic sheet was wrapped around the spooled sail, shown in the vacuum chamber in Figure 20. Strain gauges were attached to the belt, with the goal of quantifying the load placed on this restraint by the sail's decompression, but provided poor quality data in this test.

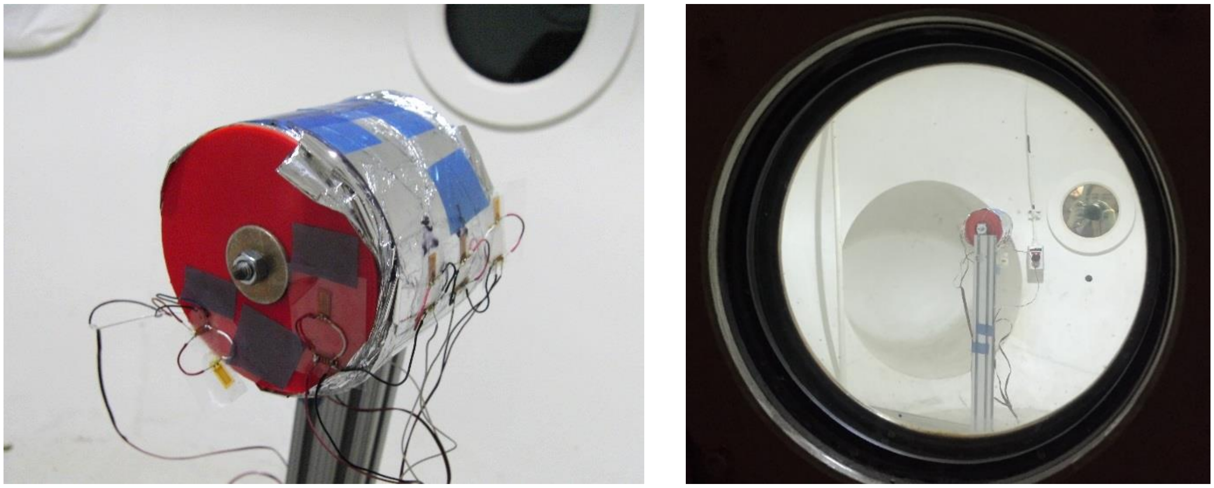

(a) (b)

Figure 20: A spooled sail in the vacuum chamber (a) and viewed through a chamber window (b). The sail on the spool consists of two quadrants, each with a long edge of 9.2 meters and a fold height of 75 mm, co-coiled on a single plastic spool. The sail was held to the spool by a clear plastic belt.

Consistent with other solar sail ascent vents tests [9] [10] [11] on z-folded and wrapped sails, ascent vent testing produced no visible change in the sail package. Specifically, no bulging, tearing, or fluttering of the edges of the packaged membrane was observed at any time during the venting process. The strain gauges installed on the belt showed inconsistent readings, with a maximum estimated belt tension of the order of 10 N occurring at the highest rate of depressurization in the test.

D. Membrane-only deployment testing

From early in development, it was assumed that the load required to deploy the membrane in space would be too low to drive any requirements on the booms or deployer. In order to confirm that this was true, and to quantify the effects of any future changes to the sail membrane, a test rig was designed to repeatably deploy the sail from its stowage container.

The pull test rig consisted of two to four 7.2-m-long rails, made of 80/20 Inc. T-slotted aluminum bars arranged as shown in Figure 21. Depending on the number of sail quadrants being deployed, different numbers of rails were used. Figure 21 shows their configuration for a two-quadrant pull test. Both continuous rails and butt-jointed discontinuous rails were used in this test without any measurable difference in performance.

Figure 22 shows the mechanism of motion for one leg of the rig. At the end of each rail was a motor-driven spool powered by a SparkFun ROB-09238 stepper motor and controlled by an Arduino microcontroller that was linked to the microcontrollers on the other rails of the rig. This spool reeled in a Kevlar string that was tied to a sliding carriage, which consisted of a linear bearing from 80/20 Inc. and an arm that supported a battery-powered wide-angle camera and a 10 lbf (45 N) Futek LRM200 load cell, pictured in Figure 23(a). This motion control system was found to be accurate enough for the test, with a discrepancy of less than 9 cm between the travel distances of the three carriages.

The load cells on the carriages were connected by long wires to a National Instruments CompactDAQ strain gauge card. One goal of the test was to plot the travel distance of the center carriage against the angle and magnitude of the load at each corner of the membrane, which required processing the video data from the carriage cameras. The travel distance of the carriage was read off the tape measure in the frame of the video (Figure 23(b)), and the angle of the load within the plane of the sail was measured from the angle of the string holding the load cell.

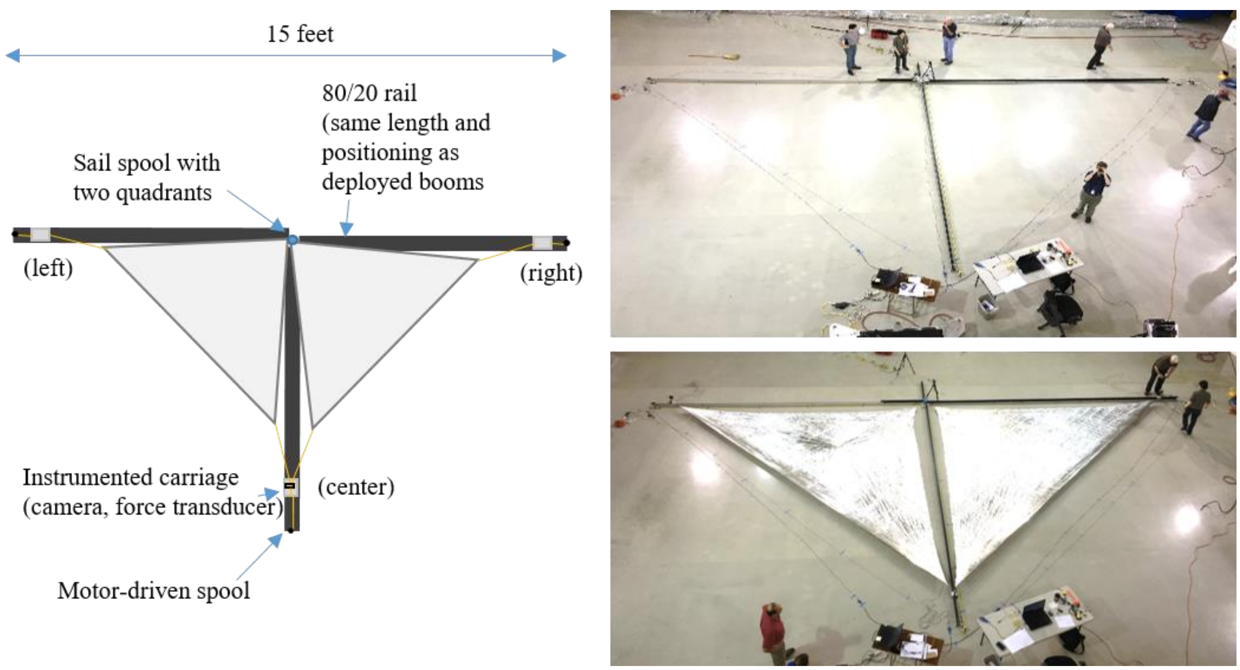

Figure 21: The sail pull test rig.

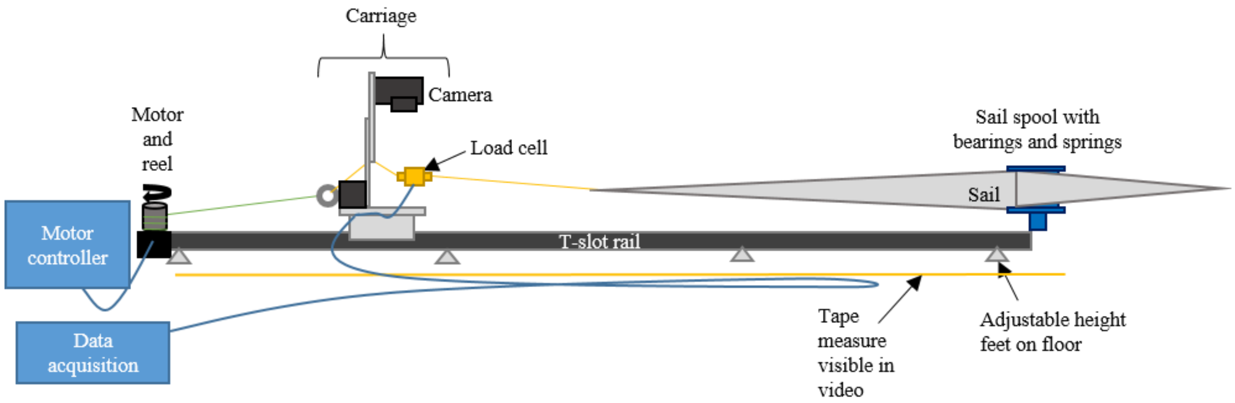

Figure 22: Side view of one leg of the sail pull test.

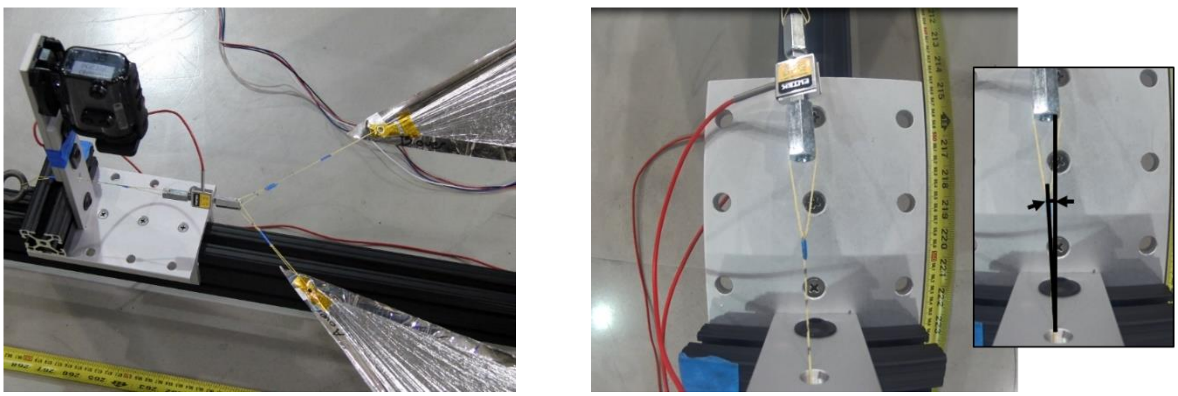

(a) (b)

Figure 23: The instrumented center carriage (a) supports the 10 lbf load cell and carries the battery-powered position camera. The view from the camera is shown in (b) (frame cropped). A tape measure was placed within the camera field of view, alongside the rail, to measure travel distance, and the in-plane angle of the net force on the two sail quadrants at this carriage was measured directly from the angle of the string in this image.

A deployment test was performed with two sail quadrants made of Mylar and seamed with pressure-sensitive adhesive tape. Still frames of video from this test are shown in Figure 24. The test had a number of goals: to identify any unexpected behaviors in the sail membrane, spool, and spring system; to establish baseline loads for deployment; and to observe the direction of the net force on the center carriage. The position versus load data for this test is shown in Figure 25, and the angle history of the load cells is shown in Figure 26. The sail design tension was 1-1.5 N, and the test loaded it beyond this range to explore the behavior of the sail and of the test rig.

The loads in Figure 25 are understood to be dominated by friction between the sail membrane and the laboratory floor, with noise from sail adhesions and the irregular motion of unfolding the sail. At the end of the membrane's deployment, the sail tension went up very quickly. When the center carriage carried 2 N of load, the sail tension was increasing by 0.3 N per cm of carriage motion, indicating that a cm-level error in manufacturing could produce a Newton-level error in sail loading, which is a high percentage of the design tension. As ACS3 development work and membrane prototyping continue, it may prove easy or difficult to size the sail and its connections to the dimensions of the booms. If it is difficult, additional springs may be added to the sail attachment points, in order to reduce the requirement of sail shape accuracy by increasing the compliance of the attachments.

During the membrane-only deployment test, it was observed that the sails were lightly stuck to themselves and to one another by adhesive along most of the taped lines of the sail, including the ripstops, edging, and some repair patches. Generally, these tacky spots released without damage to the sail, but a small number of tears observed were attributed to adhesions. In some cases, a spike in the load data was associated with an adhesion releasing in the video record, and this is believed to be the cause of most of the spikes in load. In other cases, load spikes could be connected with the sail sliding over a rail or large changes in geometry that occurred as the sail unfolded.

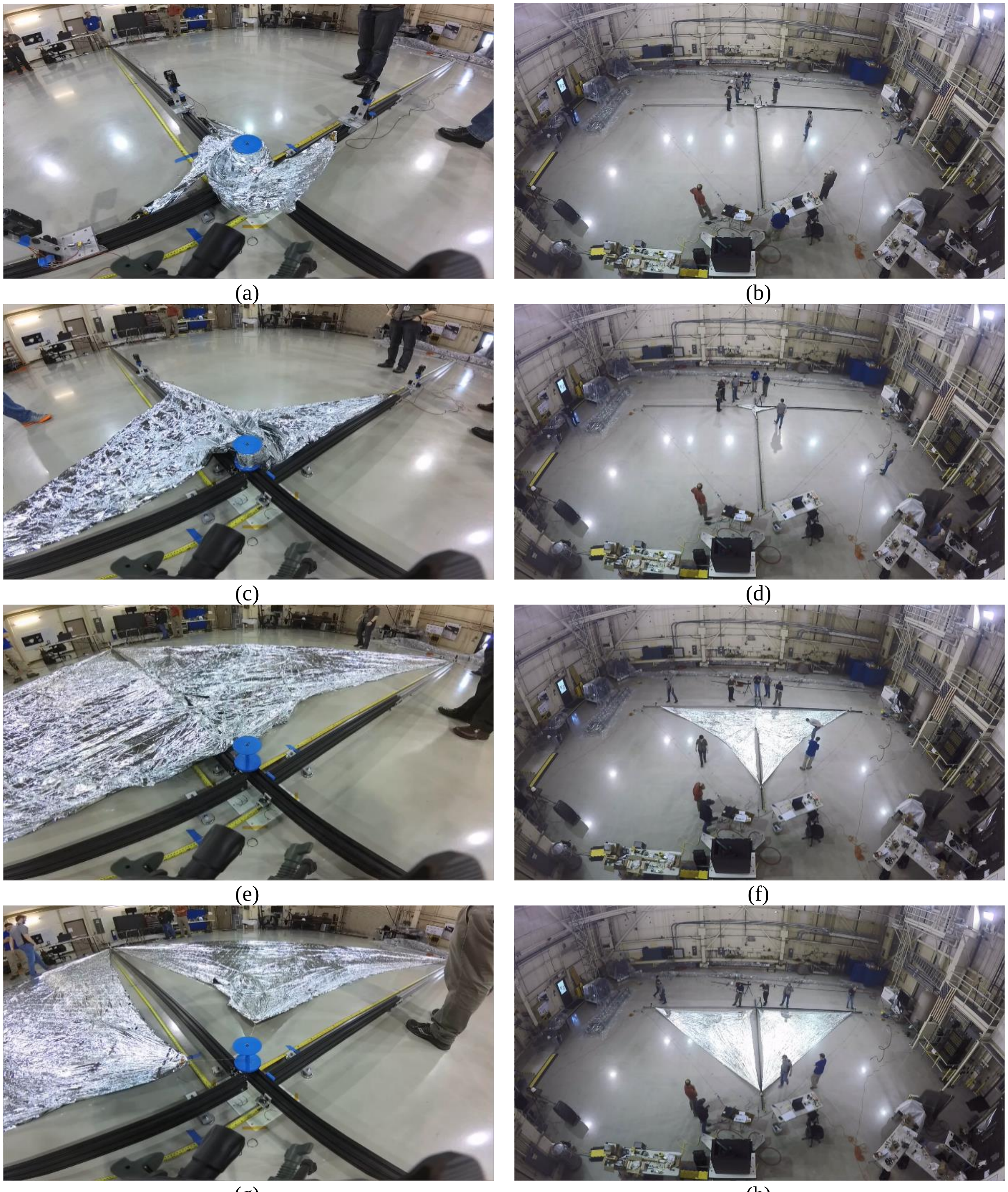

(a) (b) (c) (d) (e) (f) (g) (h)

Figure 24: A membrane-only deployment test. Early in the test, the "left" segment of sail started on the outside of the left rail (a)(b). The quadrant migrated to the correct side of the rail without intervention (c)(d). Near the end of deployment, the two sail quadrants were adhered by exposed adhesive on the edging tape (e)(f), which eventually disconnected (g)(h). Note that tears in the sail are visible in (g).

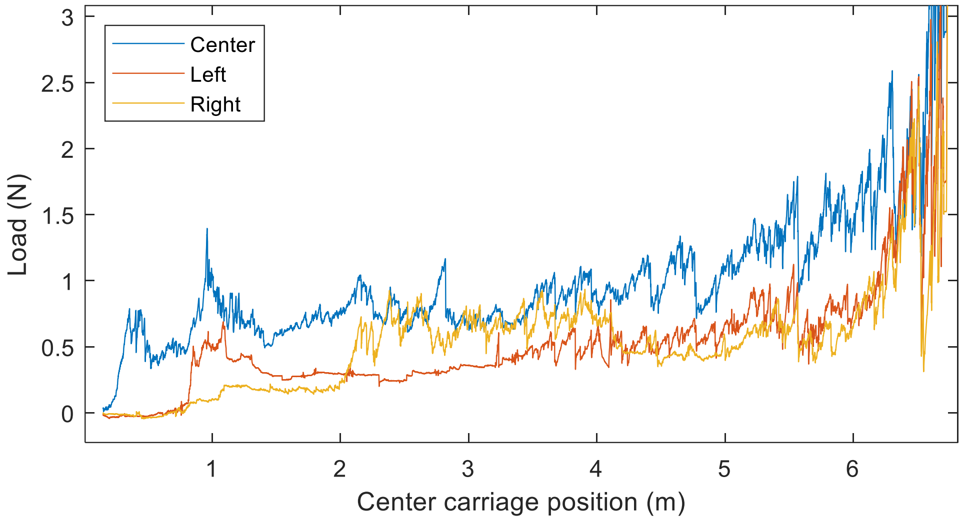

Figure 25: The sail corner loads during the membrane-only deployment test.

Both the load history and the angle history showed an event at around 0.7 m deployment that appeared in the video to be the sail sliding over the left rail of the deployment rig. This was an example of a substantial load on the booms that would not occur in space and could be reduced by gravity offloading.

Early in the test, the line angles were dependent on the sail's path as it was dragged across the floor, and varied rapidly at times due to adhesions and the low loads during sail unfolding. The angles of the loads on the left and right carriages diverged at the end of the test because the membrane became highly tensioned and these two carriages had no balancing load from adjacent quadrants. With four quadrants, the left and right carriages would be expected to experience lower line angles.

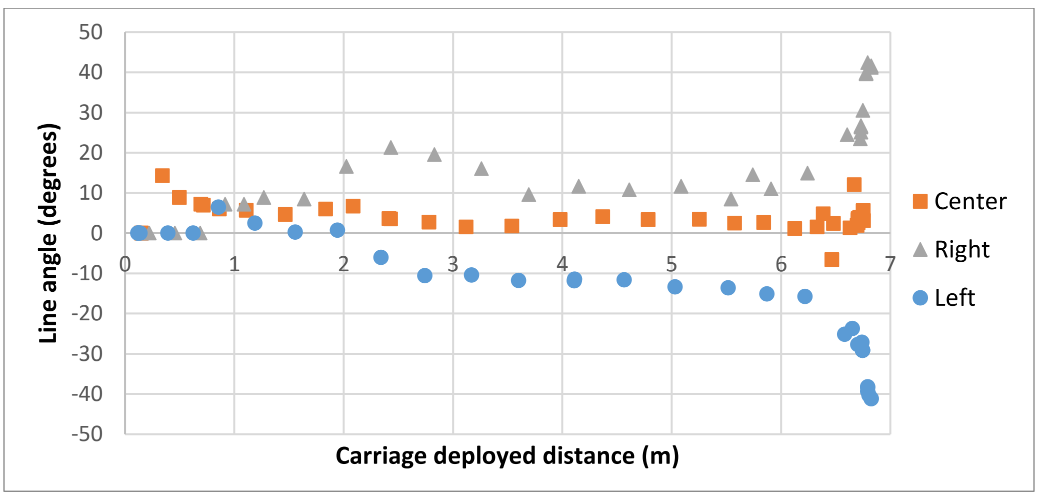

Figure 26: The observed angle of the load on each of the three carriages for the two-quadrant test.

With the benefit of this data to establish the expected range of loads and angles, the test can be improved in several ways. Chief among these is modifying the carriages so that the load cells can be mounted in a static position without off-axis loads.

V. Conclusions

We were hopeful that many of the challenges of assembling and folding prototype solar sail membranes in the lab could be overcome with enough effort and care. Through trial and error, we have found that some of these challenges are easily overcome and some require technological solutions.

Pressure-sensitive adhesive tape was found to be difficult to use with very thin membranes. It could be made acceptable by custom-manufacturing tape with overhanging backing material, or by sealing it under a layer of heat-sensitive or cured adhesive. Hot-melt polyester web adhesive was inexpensive, and was found to be easy to use and less error-prone than pressure-sensitive adhesive.

The ACS3 project settled on a partial fan folding pattern that increases the number of folds in favor of making the folded sail easier to spool. The volume efficiency of hand-wrapped sails was observed to be highly dependent upon the skill of the person or people wrapping the sail, even under artificially favorable conditions with paper models. The use of a singly folded and wrapped sail was supported by an ascent vent test that demonstrated that air was able to vent from a full-sized sail that experienced a realistic decompression profile in a vacuum chamber.

In a system with a membrane sail and slender deployable booms, coupled analysis and deployment demonstrations are crucial. It is important to understand that the booms and membranes are both very compliant, which means that fixed rails are not a perfect substitute for the booms in a sail membrane test. There are nonetheless many advantages to separating the deployment of the booms and membrane during development. With a test rig for deploying the sail membrane without the booms, it is now possible to explore several questions about the membrane. For example, this rig can distinguish between offload methods such as piping air under the membrane and attaching balloons to the membrane. It has been helpful in evaluating methods of restraining the spooled sail (for example, wrapping the spooled sail in a belt that is pulled off by the booms), because it can be quickly repeated on a smaller-scale sail. The equipment can be modified to investigate boom deployment loads, which are friction-dependent and drive deployment motor selection. Membrane development can proceed more quickly if deployment testing is separated from the booms and their deployer, so this will continue to be an important tool in sail membrane and stowage design.

Acknowledgments

The authors wish to thank Mr. Kevin Mclain (Fabrication Technology Development Branch, NASA Langley Research Center) for assistance in manufacturing the paper folding forms.

References

[1] L. McNutt, L. Johnson, D. Clardy, J. Castillo-Rogez, A. Frick and L. Jones, "Near-Earth Asteroid Scout," in *AIAA Space Conference*, San Diego, CA, 4-7 August 2014.

[2] R. Weis, "Preliminary Design and Fabrication Assessment for Two Solar Sail Candidates," ILC Dover, Frederica, Delaware, 1977.

[3] J. M. Fernandez, G. Rose, O. R. Stohlman, C. J. Younger, G. D. Dean, J. E. Warren, J. H. Kang, R. G. Bryant and W. K. Wilkie, "An advanced composties-based solar sail system for interplanetary small sail missions," in *AIAA Spacecraft Structures Conference, AIAA Scitech Forum*, Kissimmee, Florida, 2018.

[4] J. H. Kang, R. G. Bryant, W. K. Wilkie, H. M. Wadsworth, P. D. Craven, M. K. Nehls and J. A. Vaughn, "Simulated Space Environment Effects on a Candidate Solar Sail Material," in *The Fourth International Symposium on Solar Sailing*, Kyoto, 2017.

[5] M. M. Finckenor and D. Dooling, "Multilayer Insulation Material Guidelines," NASA Technical Publication TP-1999-209263, Huntsville, AL, 1999.

[6] J. M. Fernandez, V. J. Lappas and A. J. Daton-Lovett, "Completely stripped solar sail concept using bi-stable reeled composite booms," *Acta Astronautica,* vol. 69, no. 1-2, pp. 78-85, 2011.

[7] M. Arya, N. Lee and S. Pellegrino, "Wrapping thick membranes with slipping folds," in *AIAA SciTech Forum*, Kissimmee, Florida, 2015.

[8] O. R. Stohlman, M. Schenk and V. Lappas, "Development of the Deorbitsail flight model," in *Spacecraft Structures Conference, AIAA Scitech*, National Harbor, MD, 2014.

[9] T. Spröwitz and P. Seefeldt, "Qualification testing of the Gossamer-1 deployment technology," in *14th European Conference on Spacecraft Structures, Materials and Environmental Testing*, Toulouse, France, 2016.

[10] D. M. Murphy, T. W. Murphey and P. A. Gierow, "Scalable solar-sail subsystem design concept," *Journal of Spacecraft and Rockets,* vol. 40, no. 4, pp. 539-547, 2003.

[11] D. Lichodziejewski, B. Derbès, D. Sleight and T. Mann, "Vacuum deployment and testing of a 20m solar sail system," in *47th AIAA Structures, Structural Dynamics, and Materials Conference*, Newport, Rhode Island, 2006.